

Control of helicity of high-harmonic radiation using bichromatic circularly polarized laser fields

Gopal Dixit,^{1,*} Álvaro Jiménez-Galán,² Lukas Medišauskas,³ and Misha Ivanov^{2,4,5}

¹*Department of Physics, Indian Institute of Technology Bombay, Powai, Mumbai 400076, India*

²*Max-Born Institut, Max-Born Straße 2A, 12489 Berlin, Germany*

³*Max Planck Institute for the Physics of Complex Systems, Nöthnitzer Straße 38, 01187 Dresden, Germany*

⁴*Blackett Laboratory, Imperial College London, London SW7 2AZ, United Kingdom*

⁵*Department of Physics, Humboldt University, Newtonstraße 15, 12489 Berlin, Germany*

(Dated: July 17, 2018)

Abstract

High-harmonic generation in two-colour ($\omega - 2\omega$) counter-rotating circularly polarised laser fields opens the path to generate isolated attosecond pulses and attosecond pulse trains with controlled ellipticity. The generated harmonics have alternating helicity, and the ellipticity of the generated attosecond pulse depends sensitively on the relative intensities of two adjacent, counter-rotating harmonic lines. For the *s*-type ground state, such as in Helium, the successive harmonics have nearly equal amplitude, yielding isolated attosecond pulses and attosecond pulse trains with linear polarisation, rotated by 120° from pulse to pulse. In this work, we suggest a solution to overcome the limitation associated with the *s*-type ground state. It is based on modifying the three propensity rules associated with the three steps of the harmonic generation process: ionisation, propagation, and recombination. We control the first step by seeding high harmonic generation with XUV light tuned well below the ionisation threshold, which generates virtual excitations with the angular momentum co-rotating with the ω -field. We control the propagation step by increasing the intensity of the ω -field relative to the 2ω -field, further enhancing the chance of the ω -field being absorbed versus the 2ω -field, thus favouring the emission co-rotating with the seed and the ω -field. We demonstrate our proposed control scheme using Helium atom as a target and solving time-dependent Schrödinger equation in two and three-dimensions.

PACS numbers:

High harmonic generation (HHG) is an indispensable method to generate coherent, bright extreme ultraviolet (XUV) and soft x-ray radiation by up-converting intense infrared (IR) radiation via highly nonlinear process on a tabletop setup [1–7]. The generated radiation is used to interrogate ultrafast multi-electron and coupled electron-nuclear dynamics in atoms, molecules and solids [8–20]. Until very recently, isolated attosecond pulses and attosecond pulse trains were generated using linearly polarised drivers, which maximise the single-atom microscopic response. Then, however, the generated attosecond pulses are also linearly polarised. Nevertheless, generation and control of the polarisation of the harmonic radiation and consequently attosecond pulses with tunable polarisation (elliptical or circular) are highly desirable to probe chiral-sensitive light-matter interactions such as chiral recognition via photoelectron circular dichroism [21–23], discrete molecular symmetries [24, 25], x-ray magnetic circular dichroism [26, 27] and magnetisation and spin dynamics [28–31] at their intrinsic timescale.

Recent series of breakthrough experiments demonstrated generation of bright, phase-matched high harmonics of controllable polarisation [23, 26, 27, 32–35]. The scheme employs two counter-rotating circularly polarised driving laser fields with fundamental (ω) and its second harmonic (2ω). The total field has a trefoil symmetry, generating three ionisation bursts within one cycle of the fundamental field [35–39]. The resulting harmonic spectra consist of pairs of circularly polarised harmonics with alternating helicity, with orders $3N+1$ and $3N+2$, while the $3N$ orders are parity forbidden for perfectly circularly polarised drivers [34, 40–42]. The $3N+1$ harmonics co-rotate with the fundamental ω -field, while the $3N+2$ harmonics co-rotate with the 2ω -field. The ellipticity of the generated harmonics can be controlled by tuning the ellipticity of one of the driving fields [35, 43].

Extending the control of the polarisation of the high harmonics to isolated attosecond pulses and attosecond pulses in a pulse train is not straightforward. The spectrum consisting of pairs of harmonics with alternating helicity is achiral. In the time domain it yields a train of attosecond pulses with linear polarisation, rotated by 120° in each subsequent pulse. Nevertheless, it has been demonstrated that atoms with a p -type ground state (such as Neon, Argon, or Krypton gases) can lead to the generation of a chiral harmonic spectrum [39, 44–46], where the intensities of the adjacent harmonic lines with alternate helicity are substantially different. Such spectra in time domain yield elliptically polarised attosecond pulses already at the single-atom level [39]. The chirality of the spectrum from the

p -type state is attributed to the orbital angular momentum of the initial state, which in turn is related to Fano-Bethe propensity rule [47, 48].

Note that the Fano-Bethe propensity rule applies to one-photon transitions and corresponds to the recombination step of the harmonic generation process. The recombination step can not be altered by changing the parameters of the driving laser fields. However, the relative intensities of the adjacent harmonics, $3N + 1$ and $3N + 2$, can be controlled by controlling the ionisation step and the propagation of the released electron in the continuum by changing the relative intensities of the two driving fields. This opportunity was explored in Refs. [35, 44–46]. The possibility to use few-cycle driving pulses and/or change the time-delay between the two driving fields, ω and 2ω , has been explored in Refs. [35, 49]. An alternate way to induce the asymmetry in the intensities of the adjacent harmonics for p -type state is by adjusting the frequencies of the two counterrotating fields [50] or take advantage of macroscopic propagation effects, i.e., phase matching [26, 51].

In spite of this progress, one essential problem remains unresolved: the possibility to control the polarisation of isolated attosecond pulses and attosecond pulse trains generated by atoms with s -type ground state, already at the microscopic level. Here we offer a solution to this problem by showing how one can control the relative intensities of adjacent harmonic lines $3N + 1$ and $3N + 2$ for atoms with s -type ground state orbitals, such as Helium. Not only our proposal shows how one can induce asymmetry in the relative intensities of the harmonics with alternating helicity, it also shows how to enhance the intensity of the harmonics of the desired helicity selectively.

The HHG at a single-atom level is well understood using the three-step model: an electron tunnels from an atom, is accelerated by the driving field, and finally recombines with the parent ion and radiates high-energy photon [2, 3, 52, 53]. In the counterrotating bichromatic laser field, the process is controlled by the three propensity rules, one for each step: tunnel ionisation, propagation, and recombination. The control of these propensity rules offers the control over the asymmetry in the intensities of the chiral harmonics, and in turn the control over the polarisation of the resulting attosecond pulses. Our proposal relies on using a circularly polarised XUV pulse with photon energy well below the ionisation threshold to seed high harmonic generation. This scheme allows us to directly control the ionisation step and impart the desired angular momentum on the liberated electron. It also offers the added benefit of increasing the efficiency of high harmonic emission, in line with the previous works

on XUV-seeded HHG [54–59].

Control and enhancement of the efficiency of HHG using linearly polarised XUV seed and linearly polarised driving IR field have been proposed theoretically and demonstrated experimentally in Refs. [54–59]. Such combination have been used for, e.g., quantum path control [54, 55], dramatic enhancement of HHG [56], and attosecond control of ionization and HHG [57–59]. Here we extend this scheme to a circularly polarised seed XUV pulse along with bichromatic counter rotating IR driving field, showing how it allows one to control the overall helicity of high harmonic spectra. We demonstrate the viability of such control by solving the time-dependent Schrödinger equation (TDSE), in two and three dimensions. Atomic units are used throughout unless specified otherwise.

The two-dimensional TDSE (2D-TDSE) in the length gauge

$$i\frac{\partial\Phi(\mathbf{r},t)}{\partial t} = [\hat{T} + V(\mathbf{r}) + \mathbf{E}(t) \cdot \mathbf{r}]\Phi(\mathbf{r},t) \quad (1)$$

is solved numerically for a model Helium atom described by the soft-core potential [60]

$$V(\mathbf{r}) = -\frac{1}{\sqrt{\mathbf{r}^2 + a}}, \quad (2)$$

where $a = 0.2619$ is used to obtain the ionisation potential $I_p = 0.904$ a.u. for $1s$ -state of Helium. The 2D-TDSE is propagated on a cartesian grid using Taylor-series propagator with expansion up to eighth order [61]. To avoid unphysical reflections from the boundary, we used a complex absorbing potential

$$V_{\text{abs}}(x) = \eta(x - x_0)^n, \quad (3)$$

with $n = 3$ and $\eta = 5 \times 10^{-4}$. The value of the radial grid-step size and time-step size are $dr = 0.2$ a.u. and $dt = 0.005$ a.u., respectively.

The driving IR and the seed laser fields are

$$E_{\omega,\text{seed}}(t) = E_{\omega,\text{seed}} g(t) [E_x(t) \hat{x} + E_y(t) \hat{y}], \quad (4)$$

where $g(t)$ is the trapezoidal envelope with five-cycle plateau and two-cycle rising and falling edges, for $\omega = 0.05$ a.u. The magnitude of the IR field E_ω is set to 0.05 a.u. in the following.

First, we check whether the combination of a circularly polarised seed XUV pulse and a linearly polarised IR driving field leads to chiral high-harmonic spectra. The tenth harmonic, $\omega_{\text{seed}} = 10\omega$, with right-handed helicity and $E_{\text{seed}} = 0.01$ a.u. is used as a seed pulse. The

high-harmonic spectrum is shown in Fig. 1. As expected, the harmonic signal is enhanced by orders of magnitude, compared to the signal without the seed pulse (not shown), in agreement with earlier work [54, 59]. Important for us, however, is the polarisation of the generated harmonics. Fig. 1 shows that they are linearly polarised: the seed pulse does not affect the polarisation of the harmonics. The projection of the angular momentum, initially imparted on the electron by the seed pulse, is not conserved by the IR driver which is linearly polarised in the polarisation plane of the seed: the initially imparted angular momentum is ‘over-written’ by the strong driver.

We now investigate the HHG process with a bi-circular IR driving field expressed by Eq. (4) with

$$E_x(t) = \cos(\omega t) + \cos(2\omega t), E_y(t) = \sin(\omega t) - \sin(2\omega t). \quad (5)$$

Figure 2(a) shows the reference HHG spectrum for Helium in $\omega - 2\omega$ bi-circular laser fields as expressed in Eq. (5), without the seed pulse. The simulated HHG spectrum agrees well with previously reported results [26, 34, 38, 39, 62]. The harmonic lines with opposite helicity appear in pairs of equal intensity.

We now show how this result can be changed by controlling two out of the three propensity rules associated with bi-circular laser fields, studied in detail in [46]. First, we induce the chirality of the HHG spectrum by judiciously choosing the intensity ratio between the two driving fields of different colours. Figure 2(b) presents the HHG spectrum when $E_\omega = 2E_{2\omega} = 0.05$ a.u., with the rest of the laser parameters identical to those in Fig. 2(a). The total driving field still has the three-fold symmetry (inset in Fig. 2(b)), and the harmonic lines appear in pairs with alternating helicity, while $3N\omega$ harmonics are absent. The intensity of the counterclockwise rotating harmonics (red) is drastically enhanced in comparison to the clockwise rotating harmonics (blue) in the near cut-off region. This can be traced to the influence of the propagation step [46]. The $3N + 1$ lines correspond to the net absorption of $(N + 1) \omega$ photons and $(N) 2\omega$ photons, i.e., one extra photon from the ω -field. The $3N + 2$ lines correspond to the net absorption of $(N + 1) 2\omega$ photons and $(N) \omega$ photons, i.e., one extra photon from the 2ω -field. By making the intensity of the fundamental stronger, the first pathway is favoured. Recently, such control was demonstrated experimentally in Neon [46] and Argon gases [43], which have a p -type ground state and also for Helium [46], which has an s -type ground state also used in this work.

To further enhance the control of the relative intensities of the harmonic lines of alternate

helicity, we now add an XUV seed pulse: the $3N + 1 = 10$ -th harmonic, co-rotating with the ω -field. We note that this seed harmonic is about 10 eV below the ionisation threshold, and is not resonant with any excited state of the atom. The corresponding HHG spectrum, for $E_\omega = 2E_{2\omega} = 0.05$ a.u. and the 10-th harmonic with $E_{\text{seed}} = 0.01$ a.u., is presented in Fig. 2(c). Harmonic lines with unequal intensity appear in pairs of harmonics of alternate helicity and the $3N$ harmonics are forbidden. The intensity of the $3N + 1$ harmonics (red) is about two orders of magnitude higher than that of $3N + 2$ harmonics (blue), especially prominent within about the 10 harmonic orders near the seed frequency. If, on the other hand, we use the seed co-rotating with the 2ω -field, the enhancement is lost, see Fig. 2(d): the ionisation step generates electrons with the angular momentum following the 2ω -field, while the propagation step favours the ω -field.

To summarise, the use of the seed pulse co-rotating with the more intense ω driver ensures that both ionisation and propagation steps of the HHG process favour the electrons that return to the parent ion with angular momentum co-rotating with the ω -field, ensuring radiative recombination with desired helicity.

The use of 2D TDSE simulations is very useful in exploring the vast parameter space available in this problem, where one can tune the relative intensities and time-delays of the driving fields and the carrier frequency and helicity of the seed. However, the predictions of the reduced dimensionality model should be checked with full-dimensionality calculations, presented below.

The three-dimensional TDSE (3D-TDSE) is solved as described in [63]. To simulate the Helium atom, 3D single-active electron pseudo-potential is used to obtain s -symmetric ground state with $I_p = 0.9$ a.u. A small radial box of 70 a.u. is used with a uniform grid spacing of 0.02 a.u. and a complex boundary absorber at 50 a.u. The total number of points $n_r = 2500$ are used for the radial grid and the maximum angular momenta included in the expansion of the wave function was $l_{\text{max}} = 60$. The time step was set to $dt = 0.0025$ a.u.

The corresponding HHG spectrum is presented in Fig. 3. The pulse duration of 12 fs (FWHM of the intensity of a Gaussian envelope) with $\omega = 0.057$ a.u is used in 3D simulation. In the case of $E_\omega = 2E_{2\omega} = 0.05$ a.u. and with no seeding pulse (see Fig. 3(a)), the intensity of the co-rotating harmonics with the ω -field (red) is slightly stronger compared to the counter-rotating harmonics (blue). Once we add the seed, the intensity of the red lines is substantially enhanced, see Fig. 3(b). The 10-th harmonic with $E_{\text{seed}} = 0.01$ a.u is added

as seed XUV pulse. The 3D results show the same trend as the 2D calculations, but the enhancement is smaller. The same is also true for calculations for HHG from p -type state, without the XUV seed, as seen by comparing the results presented in Refs. [39, 46]: the contrast between $3N + 1$ and $3N + 2$ harmonics is higher in 2D than in 3D. We attribute this difference to stronger polarisation of the ground state in the soft-core 2D potential, with the driving ω -field already leaving its mark on the bound part of the electron wave-packet before ionisation.

In conclusion, the generation of elliptically polarised attosecond pulses and pulse trains with counter rotating bi-circular fields relies on the three propensity rules for ionisation, propagation and recombination, where only the first two can be controlled by changing laser parameters. It is known that the propensity rule for propagation can be manipulated by changing the relative intensities between the two-colour driving fields. In this work we additionally control the ionisation step by combining the co-rotating seed harmonic, which populates states that co-rotate with the fundamental driving field. By increasing the intensity of the fundamental driving field over its second harmonic, we control the propagation step, further enhancing the chance of the fundamental frequency versus its second harmonic being absorbed. Such scheme strongly favours the emission of harmonics co-rotating with the fundamental driving field and leads to chiral emission over a broad energy range of the generated harmonics.

G.D. acknowledges the Ramanujan fellowship (SB/S2/ RJN-152/2015) and Max-Planck India visiting fellowship. A.J.-G. and M.I. acknowledge support from the DFG QUTIF grant IV 152/6-1. M.I. acknowledges support from the EPSRC/DSTL MURI grant EP/N018680/1.

* gdixit@phy.iitb.ac.in

- [1] M. Ferray, A. L’Huillier, X. F. Li, L. A. Lompre, G. Mainfray, and C. Manus, *Journal of Physics B* **21**, L31 (1988).
- [2] P. B. Corkum, *Physical Review Letters* **71**, 1994 (1993).
- [3] M. Lewenstein, P. Balcou, M. Y. Ivanov, A. L’Huillier, and P. B. Corkum, *Physical Review A* **49**, 2117 (1994).

- [4] R. A. Bartels, A. Paul, H. Green, H. C. Kapteyn, M. M. Murnane, S. Backus, I. P. Christov, Y. Liu, D. Attwood, and C. Jacobsen, *Science* **297**, 376 (2002).
- [5] G. Sansone, E. Benedetti, F. Calegari, C. Vozzi, L. Avaldi, R. Flammini, L. Poletto, P. Villoresi, C. Altucci, R. Velotta, et al., *Science* **314**, 443 (2006).
- [6] P. M. Paul, E. S. Toma, P. Breger, G. Mullot, F. Augé, P. Balcou, H. G. Muller, and P. Agostini, *Science* **292**, 1689 (2001).
- [7] F. Krausz and M. Ivanov, *Reviews of Modern Physics* **81**, 163 (2009).
- [8] S. Haessler, J. Caillat, W. Boutu, C. Giovanetti-Teixeira, T. Ruchon, T. Auguste, Z. Diveki, P. Breger, A. Maquet, B. Carré, et al., *Nature Physics* **6**, 200 (2010).
- [9] S. Baker, J. S. Robinson, C. A. Haworth, H. Teng, R. A. Smith, C. C. Chirilă, M. Lein, J. W. G. Tisch, and J. P. Marangos, *Science* **312**, 424 (2006).
- [10] O. Smirnova, Y. Mairesse, S. Patchkovskii, N. Dudovich, D. Villeneuve, P. Corkum, and M. Ivanov, *Nature* **460**, 972 (2009).
- [11] W. Li, X. Zhou, R. Lock, S. Patchkovskii, A. Stolow, H. C. Kapteyn, and M. M. Murnane, *Science* **322**, 1207 (2008).
- [12] E. Frumker, C. T. Hebeisen, N. Kajumba, J. B. Bertrand, H. J. Wörner, M. Spanner, D. M. Villeneuve, A. Naumov, and P. B. Corkum, *Physical Review Letters* **109**, 113901 (2012).
- [13] G. Dixit, O. Vendrell, and R. Santra, *Proc. Natl. Acad. Sci. U.S.A.* **109**, 11636 (2012).
- [14] T. Bredtmann, M. Ivanov, and G. Dixit, *Nature Communications* **5**, 5589 (2014).
- [15] F. Lépine, M. Y. Ivanov, and M. J. J. Vrakking, *Nature Photonics* **8**, 195 (2014).
- [16] G. Sansone, F. Kelkensberg, J. F. Pérez-Torres, F. Morales, M. F. Kling, W. Siu, O. Ghafur, P. Johnsson, M. Swoboda, E. Benedetti, et al., *Nature* **465**, 763 (2010).
- [17] V. Gruson, L. Barreau, Á. Jiménez-Galan, F. Risoud, J. Caillat, A. Maquet, B. Carré, F. Lepetit, J. F. Hergott, T. Ruchon, et al., *Science* **354**, 734 (2016).
- [18] S. Ghimire, A. D. DiChiara, E. Sistrunk, P. Agostini, L. F. DiMauro, and D. A. Reis, *Nature Physics* **7**, 138 (2011).
- [19] G. Vampa, T. J. Hammond, N. Thiré, B. E. Schmidt, F. Légaré, C. R. McDonald, T. Brabec, and P. B. Corkum, *Nature* **522**, 462 (2015).
- [20] M. Garg, M. Zhan, T. T. Luu, H. Lakhotia, T. Klostermann, A. Guggenmos, E. Goulielmakis, et al., *Nature* **538**, 359 (2016).
- [21] R. Cireasa, A. E. Boguslavskiy, B. Pons, M. C. H. Wong, D. Descamps, S. Petit, H. Ruf,

- N. Thiré, A. Ferré, J. Suarez, et al., *Nature Physics* **11**, 654 (2015).
- [22] O. Travnikova, J. C. Liu, A. Lindblad, C. Nicolas, J. Söderström, V. Kimberg, F. Gel'mukhanov, and C. Miron, *Physical Review Letters* **105**, 233001 (2010).
- [23] A. Ferré, C. Handschin, M. Dumergue, F. Burgy, A. Comby, D. Descamps, B. Fabre, G. A. Garcia, R. Géneaux, L. Merceron, et al., *Nature Photonics* **9**, 93 (2015).
- [24] D. M. Reich and L. B. Madsen, *Physical Review Letters* **117**, 133902 (2016).
- [25] D. Baykusheva, M. S. Ahsan, N. Lin, and H. J. Wörner, *Physical Review Letters* **116**, 123001 (2016).
- [26] O. Kfir, P. Grychtol, E. Turgut, R. Knut, D. Zusin, D. Popmintchev, T. Popmintchev, H. Nembach, J. M. Shaw, A. Fleischer, et al., *Nature Photonics* **9**, 99 (2015).
- [27] T. Fan, P. Grychtol, R. Knut, C. Hernández-García, D. D. Hickstein, D. Zusin, C. Gentry, F. J. Dollar, C. A. Mancuso, C. W. Hogle, et al., *Proc. Natl. Acad. Sci. U.S.A.* **112**, 14206 (2015).
- [28] C. E. Graves, A. H. Reid, T. Wang, B. Wu, S. De Jong, K. Vahaplar, I. Radu, D. P. Bernstein, M. Messerschmidt, L. Müller, et al., *Nature Materials* **12** (2013).
- [29] S. Eisebitt, J. Lüning, W. F. Schlotter, M. Lörger, O. Hellwig, W. Eberhardt, and J. Stöhr, *Nature* **432**, 885 (2004).
- [30] I. Radu, K. Vahaplar, C. Stamm, T. Kachel, N. Pontius, H. A. Dürr, T. A. Ostler, J. Barker, R. F. L. Evans, R. W. Chantrell, et al., *Nature* **472**, 205 (2011).
- [31] C. Boeglin, E. Beaurepaire, V. Halté, V. López-Flores, C. Stamm, N. Pontius, H. A. Dürr, and J. Y. Bigot, *Nature* **465**, 458 (2010).
- [32] C. Chen, Z. Tao, C. Hernández-García, P. Matyba, A. Carr, R. Knut, O. Kfir, D. Zusin, C. Gentry, P. Grychtol, et al., *Science Advances* **2**, e1501333 (2016).
- [33] G. Lambert, B. Vodungbo, J. Gautier, B. Mahieu, V. Malka, S. Sebban, P. Zeitoun, J. Lüning, J. Perron, A. Andreev, et al., *Nature Communications* **6**, 6167 (2015).
- [34] A. Fleischer, O. Kfir, T. Diskin, P. Sidorenko, and O. Cohen, *Nature Photonics* **8**, 543 (2014).
- [35] Á. Jiménez-Galán, N. Zhavoronkov, M. Schloz, F. Morales, and M. Ivanov, *Optics Express* **25**, 22880 (2017).
- [36] H. Eichmann, A. Egbert, S. Nolte, C. Momma, B. Wellegehausen, W. Becker, S. Long, and J. K. McIver, *Physical Review A* **51**, R3414 (1995).
- [37] D. B. Milošević and W. Becker, *Physical Review A* **62**, 011403 (2000).

- [38] D. B. Milošević, W. Becker, and R. Kopold, *Physical Review A* **61**, 063403 (2000).
- [39] L. Medišauskas, J. Wragg, H. Van der Hart, and M. Ivanov, *Physical Review Letters* **115**, 153001 (2015).
- [40] O. E. Alon, V. Averbukh, and N. Moiseyev, *Physical Review Letters* **80**, 3743 (1998).
- [41] E. Pisanty, S. Sukiasyan, and M. Ivanov, *Physical Review A* **90**, 043829 (2014).
- [42] D. B. Milošević, *Journal of Physics B* **48**, 171001 (2015).
- [43] K. M. Dorney, J. L. Ellis, C. Hernández-García, D. D. Hickstein, C. A. Mancuso, N. Brooks, T. Fan, G. Fan, D. Zusin, C. Gentry, et al., *Physical Review Letters* **119**, 063201 (2017).
- [44] D. B. Milošević, *Optics letters* **40**, 2381 (2015).
- [45] D. Ayuso, A. Jiménez-Galán, F. Morales, M. Ivanov, and O. Smirnova, *New Journal of Physics* **19**, 073007 (2017).
- [46] Á. Jiménez-Galán, N. Zhavoronkov, D. Ayuso, F. Morales, S. Patchkovskii, M. Schloz, E. Pisanty, O. Smirnova, and M. Ivanov, *Physical Review A* **97**, 023409 (2018).
- [47] H. Bethe and R. Jackiw, *Intermediate quantum mechanics* (Westview Press, 1997).
- [48] U. Fano, *Physical Review A* **32**, 617 (1985).
- [49] M. V. Frolov, N. L. Manakov, A. A. Minina, N. V. Vvedenskii, A. A. Silaev, M. Y. Ivanov, and A. F. Starace, *Physical Review Letters* **120**, 263203 (2018).
- [50] L. Li, Z. Wang, F. Li, and H. Long, *Optical and Quantum Electronics* **49**, 73 (2017).
- [51] N. Zhavoronkov and M. Ivanov, *Optics Letters* **42**, 4720 (2017).
- [52] J. L. Krause, K. J. Schafer, and K. C. Kulander, *Physical Review Letters* **68**, 3535 (1992).
- [53] K. J. Schafer, B. Yang, L. F. DiMauro, and K. C. Kulander, *Physical Review Letters* **70**, 1599 (1993).
- [54] K. J. Schafer, M. B. Gaarde, A. Heinrich, J. Biegert, and U. Keller, *Physical Review Letters* **92**, 023003 (2004).
- [55] M. B. Gaarde, K. J. Schafer, A. Heinrich, J. Biegert, and U. Keller, *Physical Review A* **72**, 013411 (2005).
- [56] A. D. Bandrauk and N. H. Shon, *Physical Review A* **66**, 031401 (2002).
- [57] K. L. Ishikawa, E. J. Takahashi, and K. Midorikawa, *Physical Review A* **75**, 021801 (2007).
- [58] K. L. Ishikawa, *Physical Review A* **70**, 013412 (2004).
- [59] E. J. Takahashi, T. Kanai, K. L. Ishikawa, Y. Nabekawa, and K. Midorikawa, *Physical Review Letters* **99**, 053904 (2007).

- [60] I. Barth and M. Lein, *Journal of Physics B* **47**, 204016 (2014).
- [61] C. Moler and C. Van Loan, *SIAM review* **45**, 3 (2003).
- [62] S. Long, W. Becker, and J. K. McIver, *Physical Review A* **52**, 2262 (1995).
- [63] S. Patchkovskii and H. G. Muller, *Computer Physics Communications* **199**, 153 (2016).

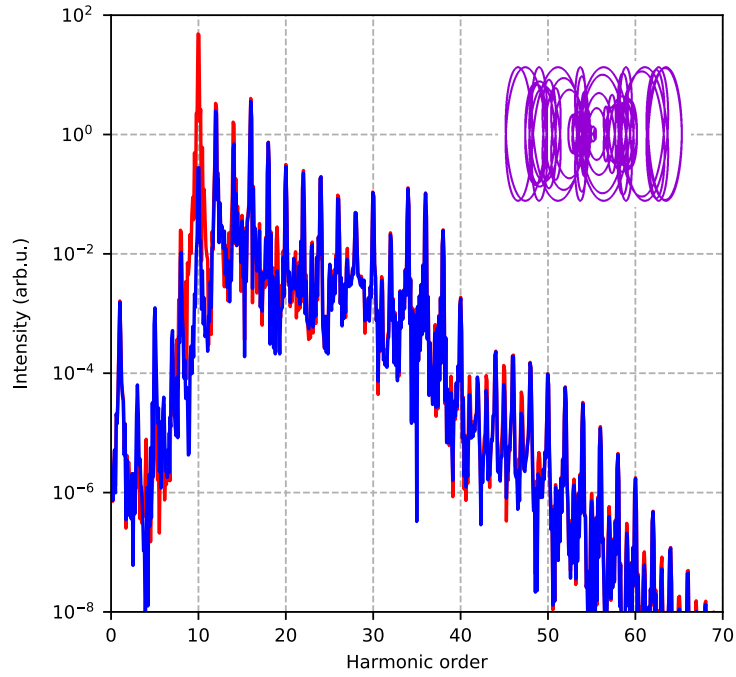


FIG. 1: High-harmonic spectrum of Helium, obtained by solving 2D-TDSE, for linearly polarised driving IR pulse in combination with right-handed circularly polarised XUV seed pulse where 10-th harmonics is used as a seed pulse. The total electric field is shown by the Lissajous figure in inset.

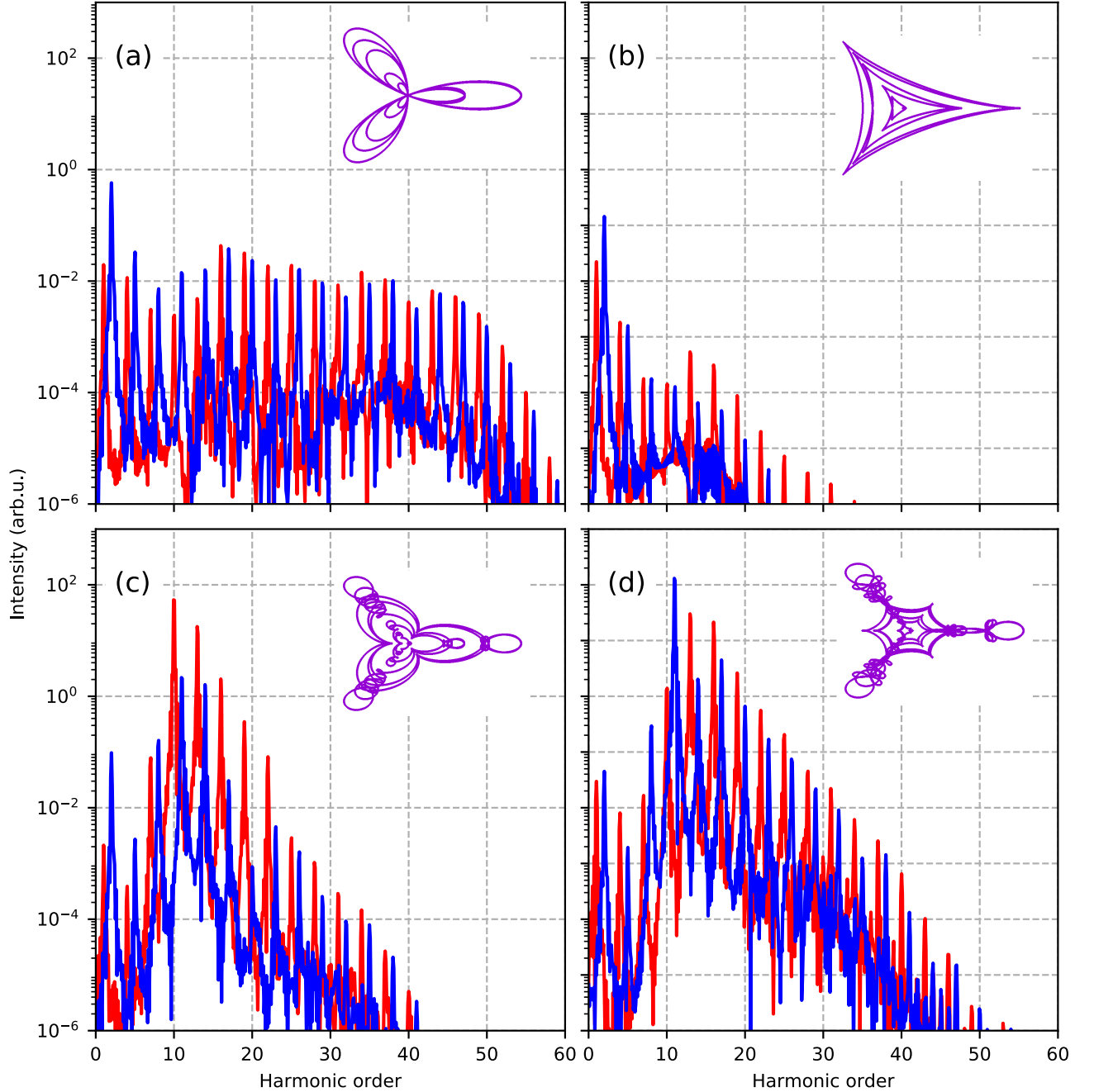


FIG. 2: High-harmonic spectrum of Helium in bi-circular driving fields obtained by solving 2D-TDSE. Spectrum with (a) $E_\omega = E_{2\omega} = 0.05$ a.u., (b) $E_\omega = 2E_{2\omega} = 0.05$ a.u., and (c) $E_\omega = 2E_{2\omega} = 0.05$ a.u., in combination with 10-th harmonic as a seed XUV pulse with right-handed circular polarisation, (d) $E_\omega = 2E_{2\omega} = 0.05$ a.u., in combination with 11-th harmonic as a seed XUV pulse with left-handed circular polarisation. The total electric field is shown in inset.

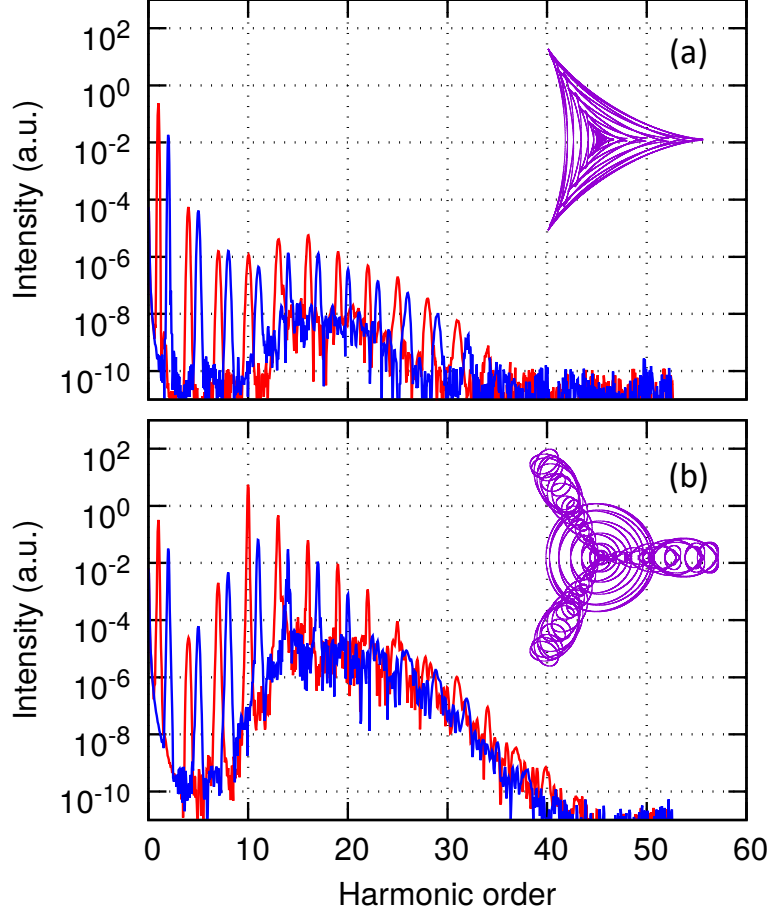


FIG. 3: High-harmonic spectrum of Helium in bi-circular driving fields obtained by solving 3D-TDSE. Spectrum with (a) $E_\omega = 2E_{2\omega} = 0.05$ a.u., and (b) $E_\omega = 2E_{2\omega} = 0.05$ a.u. in combination with 10-th harmonic as a seed XUV pulse with right-handed circular polarisation. The total electric field is shown in inset.